E171 Final Project:
Effects of Irregularities on the Dynamics of Nearly Periodic Structures

Clayson Briggs, Andres Sanchez, and Gabriel Zwillinger

I. INTRODUCTION

Periodic structures arise in various applications of structural engineering, since the manufacturing, assembly, and analysis of such structures is typically more straightforward. However, it is practically impossible to ensure that every periodic component is perfectly identical due to manufacturing or material imperfections. In periodic structures, system responses can be especially sensitive to these small inconsistencies, but often, engineers do not take this into account because it can add significant complexity to the design and analysis stages.

In this project, we model a bladed disk assembly (frequently referred to in industry as a "blisk") as a one-dimensional 50-degree-of-freedom lumped element model, shown in Figure 1. Each of the 50 blades is modeled as a mass with a material stiffness of k_0 and an aerodynamic or physical coupling stiffness of k_c. Initially, we assume that the structure is perfectly periodic, to gain a baseline understanding of the system. Then, we introduce random perturbations into the material stiffness k_0 and apply both a direct approach and a perturbation analysis to examine the perturbations' effects on the system's responses. Finally, we present a conclusion with our summary of the system and some remarks. In the end, we hope to gain intuition about the effects of various perturbations on the dynamics of periodic structures and learn more about various methods to solve eigenvalue problems in the context of structural engineering and model these perturbations.

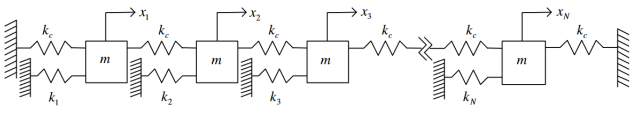

Fig. 1. A lumped element model of the bladed disk assembly [1]

II. PERFECTLY PERIODIC SYSTEM

A. Equations of Motion

To derive the equations of motion, we analyzed Free Body Diagrams (FBDs) to apply Newton's laws of motion. Because the structure is perfectly periodic, we can use symmetry to observe that only masses 1 and N are coupled to one other mass, and every other mass is coupled to two other masses. The FBD of a general case is illustrated in Figure 2.

The FBDs are summarized below:

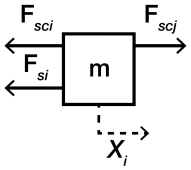

Fig. 2. The free body diagram for the i^{th} mass in the model. $\mathbf{F_s}$ represents a spring force.

For $i = 1$:

$$m\ddot{x}_1 = -k_0(x_1 - 0) - k_c(x_1 - 0) - k_c(x_1 - x_2)$$
$$\Rightarrow m\ddot{x}_1 + (2k_c + k_0)x_1 - k_c x_2 = 0 \tag{1}$$

Similarly, for $i \neq 1$ and $i \neq N$

$$m\ddot{x}_i + (2k_c + k_0)x_i - k_c x_{i-1} - k_c x_{i+1} = 0 \tag{2}$$

Finally, for $i = N$

$$m\ddot{x}_N + (2k_c + k_0)x_N - k_c x_{N-1} = 0 \tag{3}$$

For $i = 1, \ldots, N$, where $N = 50$, equations (1), (2), and (3) are collectively the Equations of Motion of the system.

B. Eigenvalue Problem

To begin the analysis and obtain the system's Eigenvalue Problem, we must first put the Equations of Motion into matrix form:

$$[M_0]\ddot{\mathbf{x}} + [k_0^*]\mathbf{x} = \mathbf{0} \tag{4}$$

where

$$[M_0] = \begin{bmatrix} m & 0 & 0 & \cdots & 0 \\ 0 & m & 0 & \cdots & 0 \\ \vdots & & & \ddots & \vdots \\ 0 & & \cdots & 0 & m \end{bmatrix}$$

and

$$[k_0^*] = \begin{bmatrix} 2k_c + k_0 & -k_c & 0 & \cdots & 0 \\ -k_c & 2k_c + k_0 & -k_c & \cdots & 0 \\ \vdots & \vdots & & \ddots & \vdots \\ 0 & \cdots & \cdots & -k_c & 2k_c + k_0 \end{bmatrix}.$$

By introducing a dimensionless stiffness ratio $R = \frac{k_c}{k_0}$, we can simplify equation (4) to:

$$\frac{m}{k_0}[I]\ddot{\mathbf{x}} + [k_0]\mathbf{x} = \mathbf{0} \tag{5}$$

where

$$[k_0] = \begin{bmatrix} 2R+1 & -R & 0 & \cdots & 0 \\ -R & 2R+1 & -R & \cdots & 0 \\ \vdots & \vdots & & \ddots & \vdots \\ 0 & \cdots & \cdots & -R & 2R+1 \end{bmatrix}$$

and $[I]$ is the identity matrix. Since we know that the solution to eq. (5) must be sinusoidal or complex exponential from the theory of Differential Equations, we can write our ansatz as:

$$\mathbf{x} = \mathbf{u}e^{j\omega_r t}.$$

where ω_r is the r^{th} natural frequency of the system. We can now substitute this into equation (5) and rearrange to obtain:

$$[k_0]\mathbf{u} = \frac{m}{k_0}\omega_r^2[I]\mathbf{u}.$$

If we introduce a dimensionless natural frequency $\overline{\omega}_r$ such that

$$\overline{\omega}_r = \sqrt{\frac{m}{k_0}}\omega_r,$$

the above reduces to our generalized eigenvalue problem for this system:

$$[k_0]\mathbf{u} = \overline{\omega}_r^2[I]\mathbf{u}. \tag{6}$$

C. Modes of Vibration

Using the generalized eigenvalue problem formulated above in equation (6), we can solve for the modes of vibration using the *eig* command in MatLab. A plot of the first five mode shapes can be seen in Figure 3 for $R = 0.01$. These five mode shapes were chosen as a representative sample of all 50 mode shapes to demonstrate the periodicity and harmonic nature of the system.

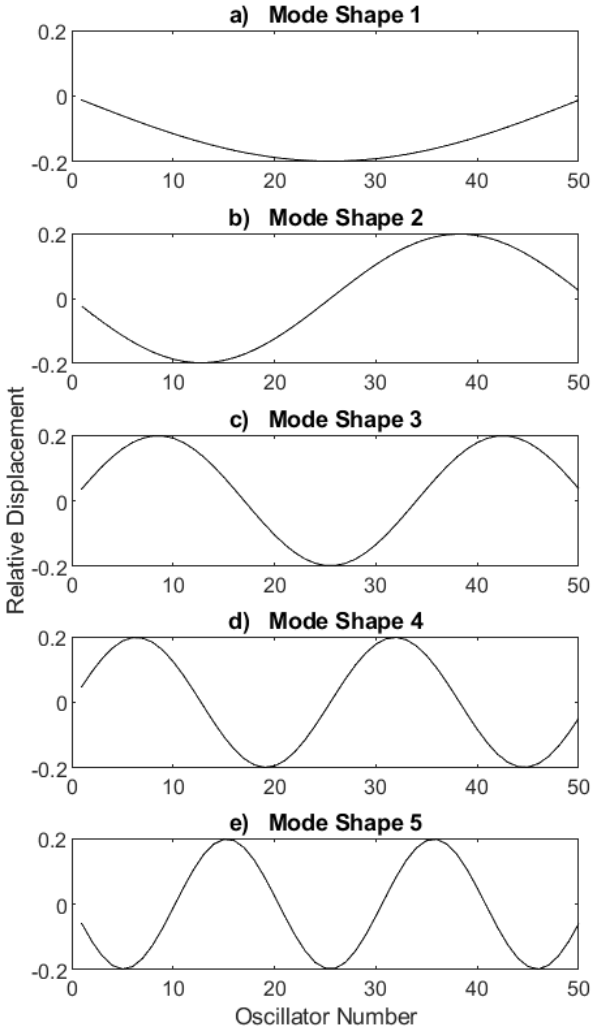

Fig. 3. First five mode shapes of the perfectly periodic system

D. Conclusion from Mode Shapes

Viewing the first five mode shapes shown in Figure 3, a clear pattern of behavior emerges. In every mode shape, the relative displacement of each mass is sinusoidal with respect to the oscillator number. Although the mode shapes are different, all demonstrate sinusoidal behavior with respect to the oscillator number. Additionally, we can see that all of the mode shapes are harmonic. The first mode shape is a sinusoid with the fundamental frequency, ω_0, and the n^{th} mode shape is a sinusoid with a frequency $n\omega_0$.

E. Coupling Ratio Effects on Mode Shapes

We can vary R and see how it impacts our mode shapes. As seen on Figure 4, two of the mode shapes for $R = 1000$ are identical to the corresponding mode shapes for $R = 1$. Plotting the rest of the mode shapes, we see that varying R has no impact on any of the mode shapes. The plots for other mode shapes were omitted as they didn't present any new information. As such, the coupling ratio R does not impact the modes of vibration for a perfectly periodic system. This makes intuitive sense when we consider the entire system because each mass is coupled with the same springs and, because there is no damping, the energy in free oscillation will be distributed evenly. As long as the masses are coupled by the same springs, R will not change the modes of vibration.

F. Frequency Response Function

The steady-state frequency response of different oscillators within the structure is important to study. If we introduce a harmonic force to the first structure,

$$F(t) = \bar{F}e^{j\omega t}$$

then the governing equation for our system becomes:

$$\frac{m}{k_0}[I]\ddot{\mathbf{x}} + [k_0]\mathbf{x} = \mathbf{F} \tag{7}$$

where

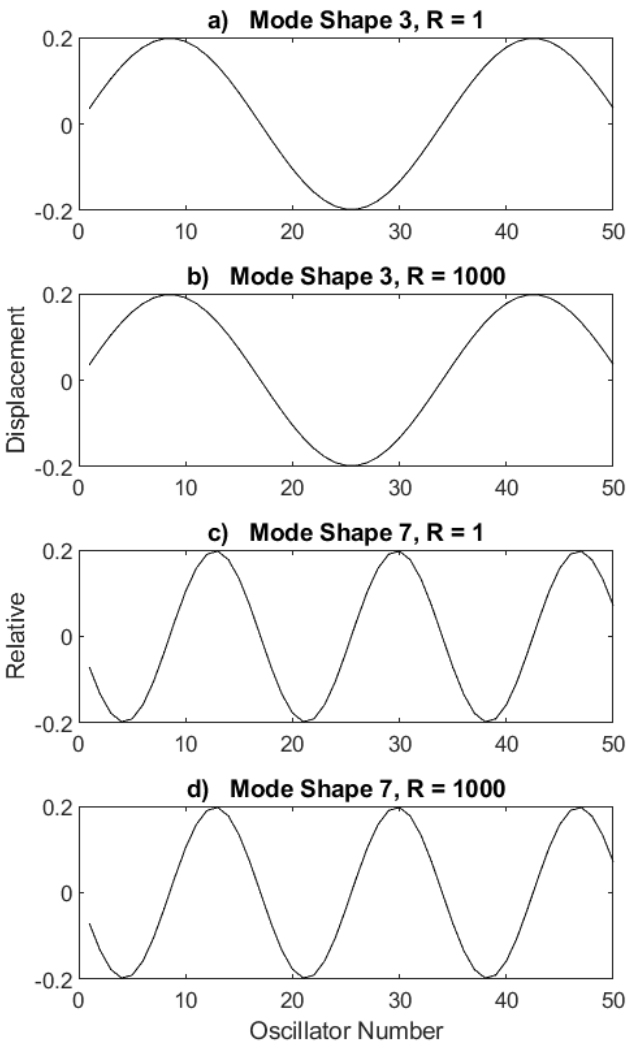

Fig. 4. A comparison of different mode shapes with varied R

$$\mathbf{F} = \begin{bmatrix} \frac{\bar{F}}{k_0} e^{j\omega t} \\ \vdots \\ 0 \end{bmatrix}.$$

From the theory of differential equations, the steady-state solution must take the form of

$$\mathbf{x} = \bar{\mathbf{x}} e^{j\omega t}.$$

We can then substitute this into eq. (5). To ensure a finite response, we also introduce a structural damping term onto the stiffness matrix, with $\gamma = 0.001$. This results in the equation:

$$\left((1+j\gamma)[k_0] - \bar{\omega}^2[I]\right)\bar{\mathbf{x}} = \frac{1}{k_0}\bar{\mathbf{F}}. \tag{8}$$

The term on the left side of this equation is our impedance matrix $[Z]$. To find the amplitude of the system's response in terms of $\bar{\omega}$, we can solve for $\bar{\mathbf{x}}$ in equation (8) using Gaussian elimination on MATLAB for a range of $\bar{\omega}$. The frequency responses for the 10th, 20th, 30th, 40th, and 50th oscillators are plotted in Figure 5 for $\gamma = 0.001$, 0.01, and 0.1.

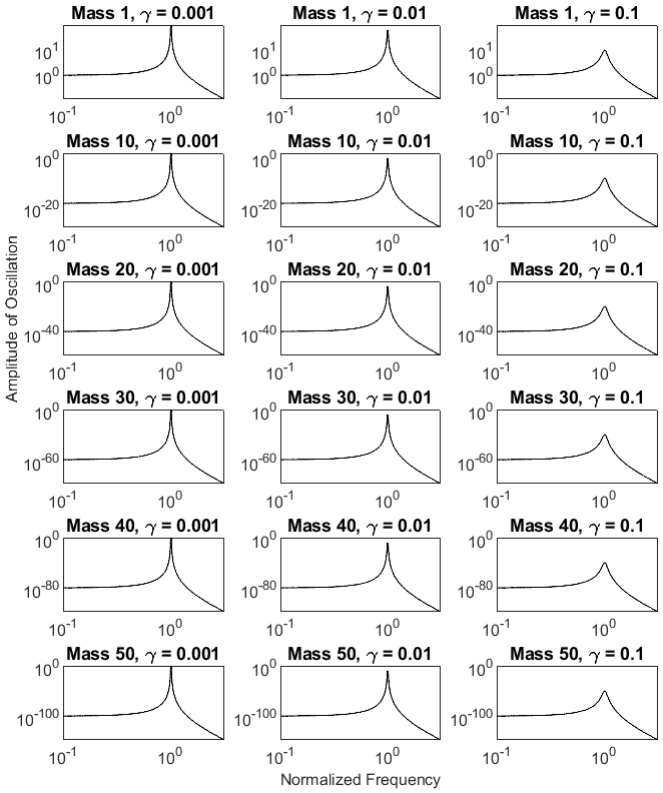

Fig. 5. The frequency responses for different oscillators and different values of structural damping

By analyzing the plot we can see that as the structural damping of the system increases, the peak amplitude of oscillation decreases. Additionally, we see that for greater oscillator numbers, the amplitude of oscillations at frequencies below the resonant frequency is lower. This makes sense because these masses are further down the chain of oscillators and there is energy loss due to damping.

This method to solve for the amplitude is known as the "impedance approach" since the matrix multiplying $\bar{\mathbf{x}}$ in equation (8) is the "impedance matrix" $[Z]$. This method is intuitive and relatively simple to understand, but $\bar{\mathbf{x}}$ must be recomputed for every value of $\bar{\omega}$, which becomes computationally expensive. Additionally, this method is only appropriate to determine the steady-state solution. This was straightforward to implement in MATLAB and the script runs quickly, so we determined that it was appropriate for acquiring the plots of Figure 5.

However, modal analysis could also be used to decouple the 50 degrees of freedom and find the amplitude of $\bar{\mathbf{x}}$ based on $\bar{\omega}$. While conceptually more challenging to understand, modal analysis can yield closed forms for both transient and steady-state solutions, and can be computationally less intensive. However, as stated previously, the impedance approach was sufficient for our purposes.

III. Nearly Periodic System

Now that we have characterized the modal response of the perfectly ordered system, we turn our attention to a non-ideal system. By varying parameters to account for irregularities, we can easily characterize a nearly periodic system instead. For the purposes of this project, we introduce a random variation in the spring stiffness k_i such that

$$k_i = k_0(1+\varepsilon\delta k_i),\ i = 1,...,N$$

where k_0 is the nominal stiffness, ε is the disorder strength, and δk_i is the random disorder parameter of the i^{th} component.

The values of δk_i are determined by generating a vector of random variables of elements x_i, with a mean of $\bar{x}$ and a standard deviation of σ. We can then create a vector of δk_i such that the mean of the set is 0 and the variance is 1 by applying the transformation

$$\delta k_i = \frac{x_i - \bar{x}}{\sigma}$$

A. Eigenvalue Problem

Now we can compute the updated system's eigenvalue problem. To do this we can perform the same steps as we did for the perfectly periodic system, but we introduce a new stiffness matrix $[k]$. Thus we obtain:

$$\frac{m}{k_o}[I]\ddot{\mathbf{x}} + [k]\mathbf{x} = \mathbf{0}$$

where

$$[k] = [k_0 + \varepsilon\delta k_i] =$$

$$\begin{bmatrix} 2R+1+\varepsilon\delta k_1 & -R & 0 & \cdots & 0 \\ -R & 2R+1+\varepsilon\delta k_2 & -R & \cdots & 0 \\ \vdots & \vdots & & \ddots & \vdots \\ 0 & \cdots & \cdots & -R & 2R+1+\varepsilon\delta k_N \end{bmatrix}$$

which allows us to write our generalized eigenvalue problem as:

$$[k]\mathbf{u} = \overline{\omega}_r^2[I]\mathbf{u}. \tag{9}$$

B. Modes of Vibration

Using the generalized eigenvalue problem in Equation 9, we can solve for the modes of vibration. First, we need to generate our mistuning parameters, δk_i. Using the transformation above, we can generate random mistuning parameters with a mean of 0 and a variance of 1. Now we will consider the case where $\varepsilon = 0.1$ and $R = 0.5$ and determine the modes of vibration for the 50 degree of freedom system. A plot of the first 5 mode shapes can be seen in Figure 6. If we compare this to our perfectly periodic mode shapes as seen in Figure 3, we can see that we no longer have perfectly periodic mode shapes. However, the overall oscillatory trends remain. We can see for the n^{th} mode shape there are n peaks. This relationship is not nearly as strong as it was in the perfectly periodic system, but it still exists. Now, let's consider the case where $\varepsilon = 0.1$ and $R = 0.01$. A plot of the first 5 mode shapes using the new parameters can be seen in Figure 7. There is a significant difference between these two cases. When $R << \varepsilon$, the mode shapes become localized. This means that instead of periodic behavior, there are large, discrete spikes. This localized behavior indicates very low coupling compared to the level of perturbation. The low coupling implies that every mass oscillates relatively independently, and the relatively large perturbations mean that each of these masses have distinct eigenvalues, resulting in the large, discrete spikes in the mode shape.

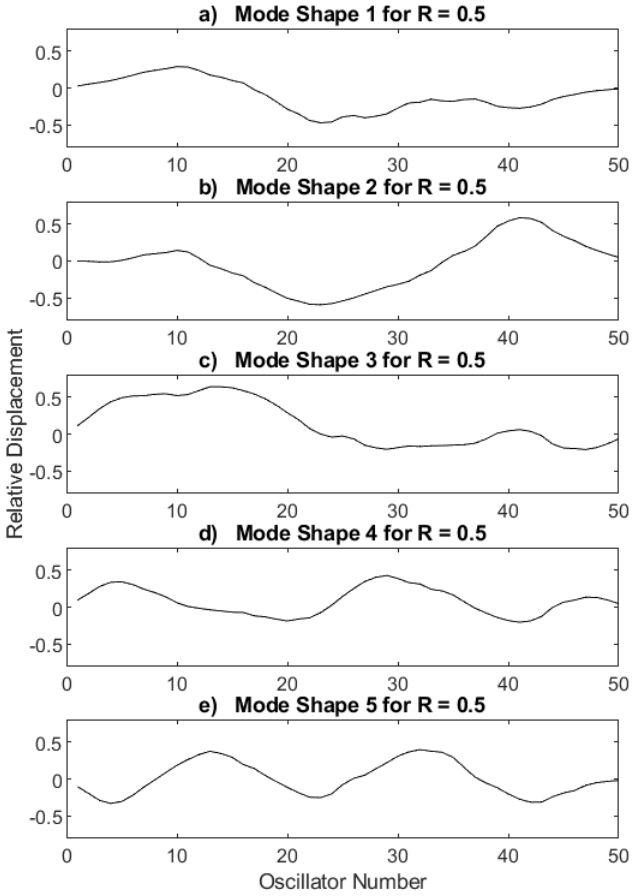

Fig. 6. The first five mode shapes for the perturbed system are plotted for $R = 0.5$.

C. Perturbation Theory

Although we can compute the eigenvalues and eigenvectors of the new, mistuned system using the generalized eigenvalue problem, we can also estimate the eigenvalues and eigenvectors using perturbation theory. Perturbation theory is beneficial because it allows us to compute the new eigenvalues and vectors without the computationally intensive task of recomputing the solutions to the GEVP. It also allows us to gain more physical insight into the system by seeing exactly

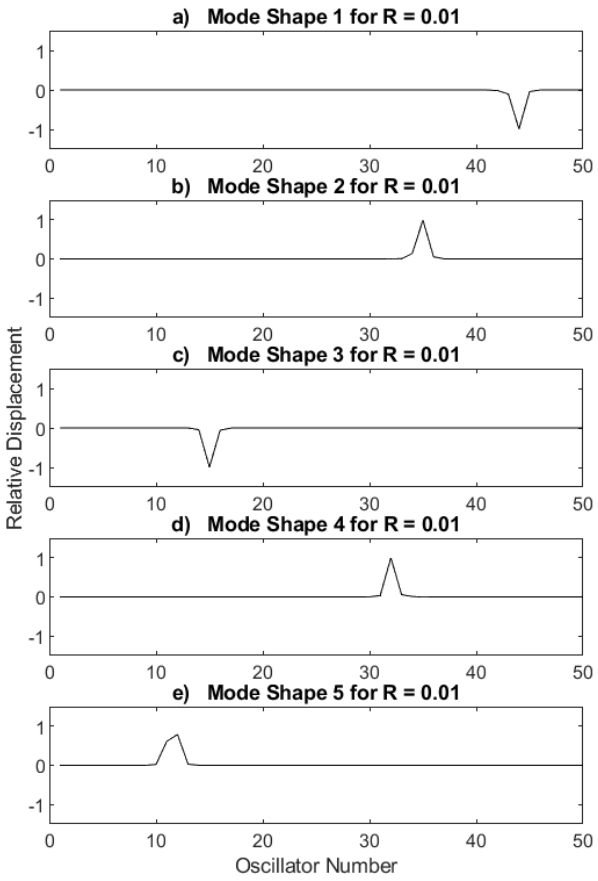

Fig. 7. The first five mode shapes for the perturbed system are plotted for $R = 0.01$.

what parameters are changing the natural frequencies and mode shapes of the system.

To compute the new eigenvalues and eigenvectors, we will utilize first-order perturbation theory. From lecture, we derived the following general equations for the eigenvalues and eigenvectors of a perturbed system.

$$\lambda_j = \lambda_{oj} + \mathbf{x}_{oj}^T([\delta k] - \lambda_{oj}[\delta m])\mathbf{x}_{oj}$$

$$\mathbf{x}_j = \mathbf{x}_{oj}(1 - \frac{1}{2}\mathbf{x}_{oj}^T[\delta m]\mathbf{x}_{oj}) + \sum_{\substack{r=1 \\ r\neq 4}}^{N}(\frac{\mathbf{x}_{or}^T([\delta k] - \lambda_{oj}[\delta m])\mathbf{x}_{oj}}{\lambda_{oj} - \lambda_{or}})\mathbf{x}_{or}$$

where λ_j is the j^{th} perturbed eigenvalue, λ_{oj} is the j^{th} unperturbed eigenvalue, $\mathbf{x}_j$ is the j^{th} perturbed eigenvector, and $\mathbf{x}_{oj}$ is the j^{th} unperturbed eigenvector.

For our system $[\delta m]$ is zero because there is no change in the mass of the blades, thus our equations simplify to:

$$\lambda_j = \lambda_{oj} + \mathbf{x}_{oj}^T[\delta k]\mathbf{x}_{oj}$$

$$\mathbf{x}_j = \mathbf{x}_{oj} + \sum_{\substack{r=1 \\ r\neq 4}}^{N}(\frac{\mathbf{x}_{or}^T([\delta k])\mathbf{x}_{oj}}{\lambda_{oj} - \lambda_{or}})\mathbf{x}_{or}$$

The $[\delta k]$ matrix is a matrix that is made up of the differences between the perturbed system and the original system. Using ε and δk_i we can compute $[\delta k]$.

$$[\delta k] = \begin{bmatrix} \varepsilon\delta k_1 & 0 & \cdots & 0 \\ 0 & \varepsilon\delta k_2 & \cdots & 0 \\ \vdots & & \ddots & \vdots \\ 0 & 0 & 0 & \varepsilon\delta k_N \end{bmatrix}$$

Finally, using our $[\delta k]$ and our equations for λ_j and $\mathbf{x_j}$ we can use MATLAB to compute new eigenvalues and eigenvectors for our system.

By varying the order of magnitude of ε and R we can see the existence of mode localization. When the order of magnitude of ε is much smaller than that of R we see periodic, harmonic behavior. A plot of the first 5 mode shapes when $\varepsilon = 0.001$ and $R = 1$ can be seen in Figure 8. In contrast, when the order of magnitude of ε is much larger than that of R we get a strong localization effect. A plot of the first 5 mode shapes when $\varepsilon = 1$ and $R = 0.001$ can be seen in Figure 9. The physical implications are that a strongly coupled non-symmetric system can handle medium to large perturbations without losing its periodicity however, a system with weak coupling can only handle very small perturbations before the mode shapes localize.

We can compare the results obtained by solving the eigenvalue problem to the results obtained by applying perturbation analysis to determine how good of an approximation perturbation analysis yields. We that the smaller our perturbations were compared to our coupling the closer our approximation was. As the perturbations compared to the coupling increased, so did the error between the approximate and directly found eigenvalues. When R = 0.5 and ε = 0.1 we had an error in our estimated eigenvalues of 0.54% When the perturbations get even smaller, and R = 0.5 and ε = 0.01 the error becomes even smaller. We have an error of only 0.0061% This shows how powerful perturbation analysis can be. Without having to resolve the eigenvalue problem we get approximations within 0.6% of the correct eigenvalue and an error even lower as the perturbations shrink. Although the approximation of our mode shapes are not quite as close as those of our eigenvalues, when we have small perturbations, the error stays under 1%. However, perturbation analysis fails when the perturbations are large compared to the coupling. For instance, if R = 0.5 and ε = 1, our percent error grows to 64.3%. This demonstrates the shortcomings of perturbation analysis. It only provides a valid approximation for medium to small perturbations with respect to the system coupling.

D. Frequency Response

Just like for the perfectly periodic system, we want to study the frequency response of each of the blades. When we introduce random variation into our system, the approach

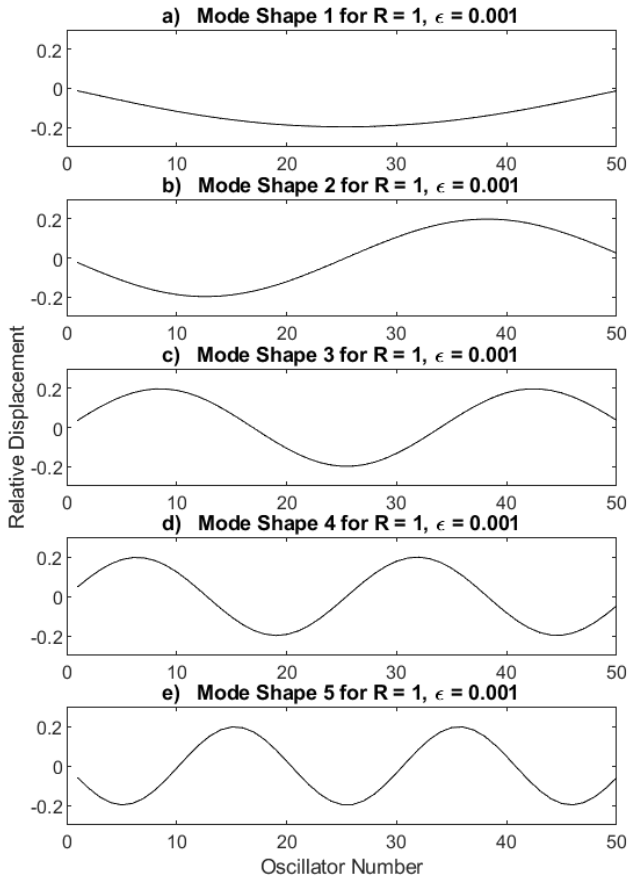

Fig. 8. The first five mode shapes for $O(R) >> O(\varepsilon)$ are displayed.

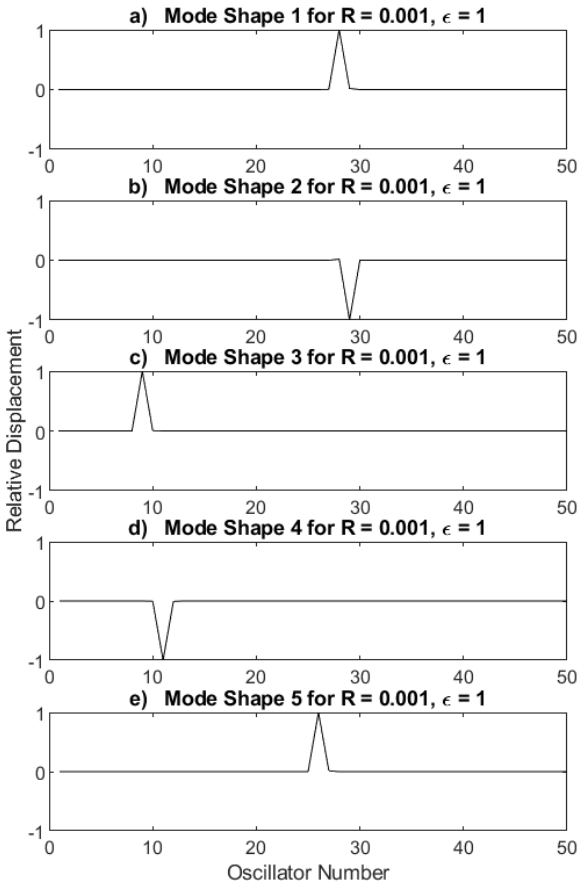

Fig. 9. The first five mode shapes for $O(R) << O(\varepsilon)$ are displayed.

for finding the frequency response doesn't change. So, we can use the same methods we used for the perfectly periodic system. After we introduce structural damping we get the following equation.

$$\left((1+j\gamma)[k]-\bar{\omega}^2[I]\right)\bar{\mathbf{x}}=\frac{1}{k_0}\bar{\mathbf{F}}. \tag{10}$$

Here, the only difference between the perturbed system and the unperturbed system is $[k]$ vs $[k_0]$. $[k]$ is the stiffness matrix of the perturbed system where

$$[k]=[k_0]+\varepsilon[\delta k]$$

Letting MATLAB solve equation 10 we get the frequency responses seen in Figure 10. Figure X shows the frequency response for the 1st, 2nd, 3rd, 4th, and 5th oscillators with structural damping of $\gamma = 0.001$ The frequency response for the perturbed system follows general second order trends like the initial tuned model. However, we note split resonances in the response magnitude, indicating the physical effects of localization.

IV. Conclusion

For this specific application, the perfectly tuned periodic system exhibits harmonic modal behavior for all N degrees of freedom in the bladed disk assembly. When introducing a structural damping term, the respective frequency response functions exhibit second order behavior, with the magnitude of the resonant peak determined by the order of the structural damping factor γ. When introducing arbitrary perturbations in the spring constants k_i, we create a mistuned periodic structure. When R is large compared to ε the mode shapes have loosely oscillatory behavior. As R decreases compared to ε, the mode shapes become localized. For the frequency response functions of the mistuned system, we still approximate second-order behavior in general trend analysis, but note split resonant peaks in the response of the individual oscillators. These split resonances could be useful in forced vibration application, as carefully mistuning the system can reduce the magnitude of the response at the system's perfectly tuned resonant peak.

Also, note that relative energy calculations can be accomplished through perturbation theory, noting that the energy of each component is proportional to its displacement squared.

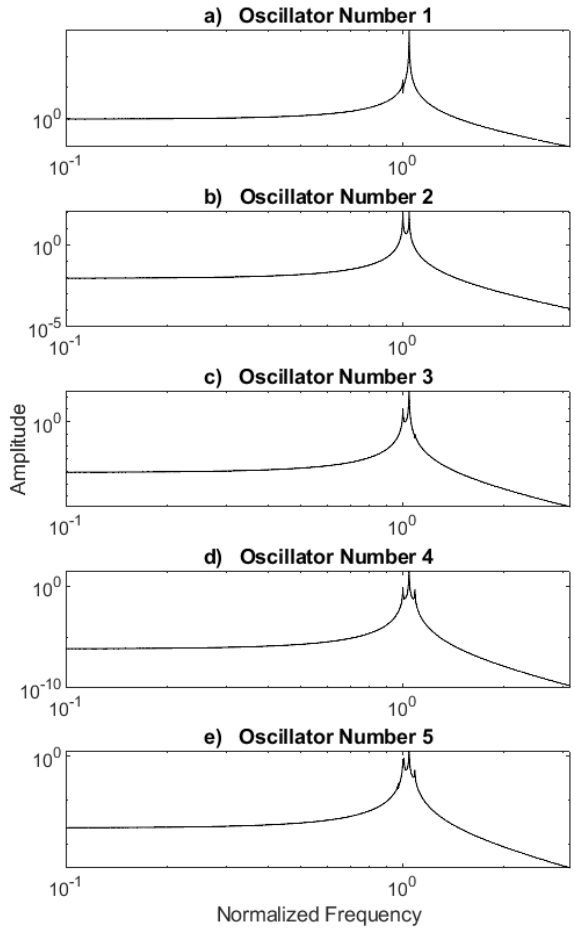

Fig. 10. The frequency responses for the first five oscillators of the perturbed slightly periodic system, $R = 0.01$ and $\varepsilon = 0.1$

In order to minimize the localization phenomena that occurs in mistuned systems, it would be ideal to introduce additional coupling in the system. By increasing the coupling in the system, the effects of R decreasing as opposed to ε are minimized. So if we rely on aerodynamic coupling, small perturbations will cause localization. However, if we introduce strong, rigid coupling between blades, then localization will not be caused by small perturbations.

This model of a bladed disk is an easy-to-understand system that allows us to model complicated system behavior and easily see the effects of perturbation analysis and coupling.

APPENDIX

The MATLAB code used to analyze this problem and generate results will be sent via email after this report is submitted.

ACKNOWLEDGMENTS

We want to acknowledge Prof. Cha for allowing us to work together on this final project, as well as for teaching us this awesome class. We've all very much enjoyed learning more about dynamics, systems, mechanics, linear algebra, and differential equations, and we all look forward to working with you more in the future and learning from you in E102!

REFERENCES

[1] Cha, P. Problem Statement for E171 Final Project, Fall 2022.